Published in final edited form as:
J Biomed Mater Res A. 2012 April ; 100(4): 918–928. doi:10.1002/jbm.a.34029.

Bone Turnover Markers Correlate with Implant fixation in a Rat Model Using LPS Doped Particles to Induced Implant Loosening[1]

Shuo Liu, **Amarjit S. Virdi**, **Kotaro Sena**, **W. Frank Hughes**, and **Dale R. Sumner***
Department of Anatomy and Cell Biology Rush University Medical Center Chicago, IL, USA

Abstract

Revision surgery for particle-induced implant loosening in total joint replacement is expected to increase dramatically over the next few decades. This study was designed to investigate if local tissue and serum markers of bone remodeling reflect implant fixation following administration of lipopolysaccharide (LPS)-doped polyethylene (PE) particles in a rat model. 24 rats received bilateral implantation of intramedullary titanium rods in the distal femur, followed by weekly bilateral intra-articular injection of either LPS-doped PE particles (n = 12) or vehicle which contained no particles (n= 12) for 12 weeks. The group in which the particles were injected had increased serum C-terminal telopeptide of type I collagen, decreased serum osteocalcin, increased peri-implant eroded surface, decreased peri-implant bone volume, and decreased mechanical pull-out strength compared to the controls. Implant fixation strength was positively correlated with peri-implant bone volume and serum osteocalcin and inversely correlated with serum C-terminal telopeptide of type I collagen, while energy to yield was positively correlated with serum osteocalcin and inversely correlated with the number of tartrate resistant acid phosphatase positive cells at the interface and the amount of peri-implant eroded surface. There was no effect on trabecular bone volume at a remote site. Thus, the particle-induced impaired fixation in this rat model was directly associated with local and serum markers of elevated bone resorption and depressed bone formation, supporting the rationale of exploring both anti-catabolic and anabolic strategies to treat and prevent particle-related implant osteolysis and loosening and indicating that serum markers may prove useful in tracking implant fixation.

Keywords

Loosening; Polyethylene particles; Implant fixation; histomorphometry; Serum biomarkers

[1]No benefit of any kind will be received either directly or indirectly by the author(s).

*Correspondence to Dale R. Sumner Department of Anatomy and Cell Biology Rush University Medical Center 600 South Paulina Street, Rm 507 Chicago, IL, 60612 Tel: 312-912-5511, Fax: 312-942-5744, rick_sumner@rush.edu.
Current addresses of other authors:
Shuo Liu: Department of Orthopaedic Surgery, School of Medicine, Johns Hopkins University, 720 Rutland Avenue, Ross Building #229, Baltimore, MD 21205
Amarjit S. Virdi: Department of Anatomy and Cell Biology, Rush University Medical Center, 600 South Paulina Street, Rm 507, Chicago, IL, 60612
Kotaro Sena: Department of Anatomy and Cell Biology, Rush University Medical Center, 600 South Paulina Street, Rm 507, Chicago, IL, 60612
W. Frank Hughes: Department of Anatomy and Cell Biology, Rush University Medical Center, 600 South Paulina Street, Rm 507, Chicago, IL, 60612

CONFLICT OF INTEREST

The authors confirm that there are no known conflicts of interest associated with this publication and there has been no significant financial support for this work that could have influenced its outcome.

INTRODUCTION

Aseptic loosening, which is often associated with peri-prosthetic osteolysis, is recognized as one of the primary causes of failure in total hip and knee arthroplasty. The annual incidence of hip and knee revision procedures in the US is projected to increase by 137% and 601%, respectively, from 2005 to 2030 [1]. Many of these procedures are performed because of loss of implant fixation. Thus, the need to develop prevention and/or treatment strategies for osteolysis and aseptic loosening is becoming urgent.

A commonly cited mechanism of osteolysis is that wear debris derived from the prosthesis activates macrophages and monocytes to release pro-inflammatory cytokines, which subsequently increase the activity of osteoclasts and cause bone loss, eventually leading to implant loosening [2–4]. To our knowledge, extant animal models lack quantitative information on the effect of particles on bone formation and bone resorption in the peri-implant region. In addition, the effect of particles on serum biomarkers of bone turnover has not been studied in any animal model of implant loosening.

Adherent endotoxin increases the bioreactivity of particles in vitro and leads to more osteolysis in vivo [5,6]. Furthermore, endotoxin-free particles implanted in vivo soon accumulate endotoxin and particles with high levels of adherent endotoxin lose the vast majority of the endotoxin which then accumulates locally in fibrous tissue adjacent to the implantation site, suggesting that the level of adherent endotoxin may be regulated [5].

Several criteria have been used to characterize osteolysis and aseptic loosening, some of which have been replicated in animal models. For instance, radiolucent zones around the implant have been well described in patients with loose prosthetic components [7] and animal models [8]. Reduction in peri-implant bone volume has been reported in patients with problematic arthroplasty [9] and has been used to validate animal models of osteolysis [10,11]. There have not been studies in these models of the architecture of the peri-implant trabecular bone nor have there been reports on changes in bone surface characterization following administration of particles. The presence of a synovial-like membrane at the bone-implant interface is a pathological feature of osteolysis [12], and has also been included in the evaluation of animal models [8,13,14]. In addition, implant migration in clinical cases is a sign of aseptic loosening [15], and has been assessed in terms of implant fixation strength in animal models [11,16,17]. There are several other criteria that have not been emphasized, but may prove to be important in the study of implant loosening and osteolysis. Biomarkers of bone resorption and formation have been investigated in patients with poorly fixed implants or peri-prosthetic osteolysis [18–23]. In general, biomarkers of bone resorption are elevated, but changes in biomarkers of bone formation are inconsistent. In osteolysis, biomarkers have not been studied in animal models of implant fixation.

Here, we tested the hypothesis that administration of endotoxin-adherent polyethylene particles alters serum and histologic markers of bone formation and resorption in a rat model of intra-medullary implantation. Furthermore, we sought to determine if these markers were correlated with assessments of implant fixation. We used endotoxin ‘contaminated’ particles to maximize the biological response. We found that markers of bone resorption were inversely correlated with fixation endpoints, while markers of bone formation were positively correlated with these endpoints and that the peri-implant trabecular bone volume was positively correlated with implant fixation. The model displayed other characteristic features of particle induced osteolysis such as the presence of a synovial-like membrane, radiolucencies at the bone-implant interface, and depressed peri-implant bone volume. We also found that trabecular bone volume at a remote site was not affected by the treatment, suggesting that local injection of the particles did not have a systemic effect on the skeleton.

Thus, the present study provides the first data in a rat implant model that mechanical fixation is correlated with serum and peri-implant histomorphometric markers of bone formation and resorption.

MATERIALS AND METHODS

Experimental design

This study was approved by the local Institutional Animal Care and Use Committee. NIH guidelines for the care and use of laboratory animals (NIH Publication #85-23 Rev. 1985) were observed. Twenty-four male Sprague-Dawley rats (400–425g, Harlan, Indianapolis, IN, US) received bilateral femoral implants. From the first day post-surgery, 12 animals were randomly selected to receive weekly bilateral intra-articular injections in each knee of lipopolysaccharide (LPS)-treated polyethylene (PE) particles in 6% rat serum vehicle, while the remaining 12 rats received injections of vehicle alone as a control. The sample size of 12 per group was chosen to have adequate power (beta = 0.80 at an alpha level of 0.05) to detect differences on the order of 25% in the pull-out strength based on previous studies in our lab of implant fixation in the rat model. After 12 weeks, all animals were euthanized. Femurs were carefully dissected without disturbing the joint surface. Left femurs were fixed in 10% neutral buffered formalin at 4°C for contact radiography, μCT and histology. Right femurs were wrapped with saline-soaked gauze and frozen at −20°C for contact radiography, μCT and mechanical pull-out testing. In a second group of 24 rats divided equally between control and LPS-doped particle injected animals, we examined the bone of the proximal humerus to determine if there were any remote effects on trabecular bone volume.

Implants

15 mm long by 1.5 mm diameter titanium rods (99.6% in purity, Goodfellow, Oakdale, PA, US) were sonicated in hexane, methanol, acetone and water for 15 minutes each, followed by dual acid etching [24]. Implants were sterilized in 70% ethanol over night. After drying at room temperature, the implants were kept in sterile saline until surgery in order to prevent oxidation.

Particles

PE particles (mean of 1.75 ± 1.43 μm and median of 1.42 μm) were used in this study (Ceridust VP 3610, Clariant, Coventry, RI, USA). The particles were sterilized in 70% ethanol for 24 hours. To increase the bioactivity of the particles, they were then incubated in 0.78 μg/ml LPS from *Escherichia coli* (L4516; Sigma-Aldrich, St. Louis, MO, US) for 24 hours at room temperature. Then, the particles were washed with PBS 3 times to remove unbound LPS. The activity of LPS on the surface of the particles was tested by the Limulus Amebocyte Lysate test (Lonza Walkerville Inc, Walkerville, MD, US) at room temperature [25]. The activity of LPS on the surface of LPS-treated PE particles was 6.85 EU/10^7 particles, which was 23 times greater than the activity of non-LPS-treated PE particles. The LPS-doped particles were suspended in sterile PBS to make a final concentration of 9.38×10^9 particles/ml in 6% rat serum (Ab7488, Abcam, Cambridge, MA, US) in sterile phosphate buffered saline (PBS). The particles were aliquoted and stored in sterile vials at −20 °C until use. Each injection had a volume of 50 μl (4.69×10^7 particles). Each animal in the particle group received 4.69×10^7 particles x 2 knees x 12 weeks for a total of 1.1256×10^{10} particles. The total EU received was 6.85 EU/10^7 particles × 1.1256×10^{10} particles = 7710.36 EU. Thus, because 1 EU corresponds to 10^{-10} g of LPS [26], each rat received 7.71036×10^3 EU x 10^{-10} g/EU LPS = 7.71036×10^{-7} g LPS ≈ 0.77 μg LPS.

Surgical procedure

All the rats received bilateral intramedullary implantation of the titanium implants under anesthesia of ketamine (100 mg/kg, i.p.) and xylazine (5 mg/kg, i.p.). After shaving and scrubbing with betadine and alcohol, each knee was incised on the medial side of patellar tendon to expose the joint surface. A Dremel drill bit, 1.6 mm in diameter, was used to penetrate the inter-condylar notch. Then, a hand drill, 1.5 mm in diameter, was used to ream the bone marrow to create a 15 mm long canal from the joint surface. Another hand drill, 2.0 mm in diameter, was used to enlarge the distal 5mm of the canal. The site was irrigated with saline. An implant was placed into the canal with the proximal 10 mm of the implant press fit in the femoral bone marrow cavity and the distal 5 mm of the implant surrounded by a 0.25 mm gap (Fig. 1). The incision was closed by nylon suture and protected by stapling.

Bacteriological test

To collect samples for bacteriology, the knee joint was exposed under sterile condition just after the animals were sacrificed. A swab sample of the femoral surface was collected from both the medial and lateral femoral condyles. Bacteriological tests for aerobic and anaerobic microorganisms were performed in a core facility (Department of Pathology, Rush University Medical Center, Chicago, IL, US).

Contact radiography

The retrieved femurs were contact radiographed (MX-20, Faxitron X-ray, Lincolnshire, IL, US) at 30kV for 15 seconds using medial-lateral and cranial-caudal projections. The presence or absence of radiolucent zones around the implant was examined by two reviewers independently.

μCT

Femurs were scanned perpendicular to the long axis of the implant at 70 kVp, intensity 114 μA, 300-ms integration time with 30μm isotropic voxels (Scanco μCT 40, Wayne, PA, USA). Femurs for histology were scanned in 10% neutral buffered formalin, while femurs for mechanical testing were first thawed and scanned in saline. On the scout view, the distance from the distal end of the implant to the articular surface of the distal femur was measured to define the location of the implant. Three consecutive regions of interest (ROIs), each of which covered 3 mm lengths of the implant, were selected. The most distal region of interest (ROI III) started from the level of the growth plate. Total volume was defined as the region between the endocortical surface and 48 μm away from the implant surface to avoid metal-induced artifacts in the images [27]. Images were processed by a bone Gaussian filter σ=1.5 support=2 and a titanium Gaussian filter σ=2 support=2. The bone volume per total volume (BV/TV), connectivity density (Conn.D.), bone surface per bone volume (BS/BV), trabecular number (Tb.N), trabecular thickness (Tb.Th), and trabecular separation (Tb.Sp) were determined at all 3 ROIs using the manufacturer's software at a threshold of 250. Nomenclature followed recently established guidelines [28]. Three-dimensional renderings were created using the manufacturer's software. The 24 humeri from the second experiments were scanned by μCT as described above. We determined trabecular BV/TV for a defined region of interest in the proximal aspect of each humerus.

Histology

Samples were decalcified in 10% ethylenediaminetetraacetic acid for 3 weeks at room temperature. The proximal aspect of the femur was removed without disturbing the implant. Then, the implant was carefully located and removed, and the samples were dehydrated and embedded in paraffin according to routine methods. From the resulting block, 7 μm thick sagittal sections were cut parallel to the long axis of the femur using a microtome (RM 2255,

Leica, Houston, TX, USA) and mounted on slides for hematoxylin and eosin (H&E) staining. Histological structure was evaluated with light and polarized light microscopy (Nikon Eclipse 80i, Nikon Instruments Inc., Melville, NY, USA). Static bone histomorphometry was evaluated with the aid of a Merz grid at 200X magnification. The ROI for static histomorphometry began 500 μm proximal to the distal growth plate, and extended proximally for 5 mm and included the area between the implant surface and endocortical surface. We determined eroded surface per bone surface (ES/BS), osteoblast surface per bone surface (Ob.S/BS), quiescent surface per bone surface (QS/BS) and bone volume per total tissue volume (BV/TV) [29]. Other paraffin sections were prepared for tartrate resistant acid phosphatase (TRAP) staining following the manufacturer's protocol (Sigma-Aldrich, St. Louis, MO, US). Each sample was counter stained with methyl green. The number of TRAP positive cells along the length of the implant-facing bone surface at the bone-implant interface was counted on two slides.

Mechanical pull-out testing

The strength of implant fixation with the host bone was measured by a mechanical pull-out test. To prepare each specimen, the distal 10–12 mm of the femur was encased in dental acrylic (Lang Dental, Wheeling, IL, US). Using the medial-lateral x-ray image as a guide, the level of the proximal end of the implant was located within each femur. The cortical bone was carefully transected without touching the implant 4–5 mm distal to the proximal end of the implant by using a precision saw (Isomet Low Speed Saw, Buehler, Lake Bluff, IL, US). Then, the proximal aspect of the femur was carefully removed to expose the proximal 25–30% of the implant (4.22 ± 0.88 mm). The exposed implant was gripped, and a S hook was placed at the distal end of the specimen to permit coaxial alignment of the implant in the direction of the applied force. Pull-out testing was conducted at a displacement rate of 0.25 mm/min to failure (Instron 8847 testing System, Instron, Canton, MA, US) [30,31]. Pull-out strength was calculated by dividing the force (N) at the point of failure by the surface area of the implant in contact with tissue (mm^2). Energy to yield (N-mm) and energy to failure were calculated as the area under the load-displacement curve until the yield point or failure point, respectively. Stiffness (N/mm) was calculated as the slope of the linear portion of the load-displacement curve before the yield point.

Serum biomarkers

Blood samples were collected through cardiac puncture at sacrifice and centrifuged at 2,000 rpm for 5 min at 4 °C to separate the serum. Levels of osteocalcin (OC) and C-terminal telopeptide of type I collagen (CTX-I) in the serum were measured by using rat-specific sandwich enzyme-linked immunosorbent assay kits (Immunodiagnostic System Inc., Fountain Hill, AZ, USA). All samples were diluted appropriately to fall in the standard curve range and were assayed in duplicate.

Statistics

SPSS for Windows (Version 15) was used for statistical analysis. Nonparametric statistical methods were used, including the Mann-Whitney test to compare the particle-treated and control groups with respect to continuous variables, and the chi-square test of association and Fisher's exact test to compare the groups with respect to percentages. Scatterplots and Spearman correlations were obtained to investigate relationships between non-categorical variables. A 0.05 significance level was used for all statistical tests. Since there were multiple comparisons within each group of variables, we adjusted the significance level using the Bonferroni method (i.e., 0.05/n, where n = the number of comparisons within each group of variables). For instance, for the weight data, there were three comparisons, so the adjusted p value to achieve significance was 0.05/3 = 0.017. Data are presented as mean (± standard deviation). Due to technical errors in some assays, the sample sizes available for

statistical analysis were less than the original sample size of 12 per group. Therefore, for each endpoint we explicitly list the sample size used in the statistical analysis.

RESULTS

Weight gain

There was no difference between the particle-treated and control groups with respect to weight at the start of the study and both groups had a significant increase in weight during the 12 week experimental period (Table 1). The particle-treated group had significantly lower weight gain beginning at six weeks than the control group (Fig. 2).

Gross observation on knee joints and bacteriological tests

The control rat knee joints appeared to be unaffected by weekly vehicle injections. The knee joints of all particle-treated rats were noticeably swollen compared to the control animals. The joint capsules of all particle-treated rats were thicker than those from control animals. Some granulation tissue was present in the joint capsule of 2 particle-treated rats. The articular surface of knees from all particle-treated rats was not smooth. Two of the particle-treated rats had areas of erosion to the subchondral bone. The bacteriological tests were negative for aerobic and anaerobic microorganisms in both groups.

Contact radiography

A radiolucent region adjacent to the implant surface was detected at the distal one-third of the implant in 91.7% (11/12) of the particle-treated group and 25.0% (3/12) of the control group ($p = 0.001$, Fig. 3).

μCT

The location of the implant from the distal-most aspect of the bone was 4.3 ± 1.8 mm in the particle-treated group and 4.7 ± 0.8 mm in the control group ($p = 0.73$). Inspection of 3-dimensional renderings gave a clear impression of less peri-implant bone volume adjacent to the distal one-third of the implant (Fig. 3). Within the distal region of interest, the particle-treated group had 45% lower BV/TV ($p=0.001$) and 63% lower Conn.D. ($p=0.001$) (Table 1). In addition, there was 17% lower Tb.N ($p=0.043$) and 22% higher Tb.Sp ($p=0.018$), but these p values did not reach significance after Bonferroni adjustment for multiple comparisons ($p < 0.01$, since there were five comparisons of interest in this group of variables). There was no difference in Tb.Th. No significant differences were found between the particle-treated and control groups with respect to bone parameters at the proximal two regions of interest.

In the humerus, the BV/TV in the control group was 9.2% (± 2.1%) and the LPS-doped PE group was 10.8% (± 4.6%). This difference was not significant ($p = 0.583$, $n = 12$ per group).

Mechanical pull-out testing

The particle-treated group had significant 41% lower fixation strength ($p<0.001$) and 51% lower energy to yield ($p=0.004$) (Table 1). Neither the 47% lower interface stiffness ($p=0.028$) nor the 43% lower energy to failure ($p=0.053$) in the particle treated group compared to the control group were significant using the Bonferroni adjusted significance level of $p < 0.0125$ (i.e., 0.05/4, since there were four comparisons of interest).

Histology

Synovial-like tissue covered the surface of the articular cartilage of the distal femur in all samples from the particle-treated group, but not in the control group (Fig. 4). Similar tissue, which consisted of a synovial-like layer of lining cells and multiple layers of fibrocytes associated with macrophages, was also observed at the bone-implant interface close to the distal end of the femur in 7 samples from the particle-treated group (Fig. 5A and 5C), but none of the control group. Under polarized light, many intracellular birefringent particles were detected in this tissue and to a lesser degree in the bone marrow space in the particle-treated samples (Fig. 5B and 5D). In the control group, a thick and even layer of peri-implant bone was present around the implant (Fig. 5E and 5F) with lack of birefringent particles.

Of the static histomorphometry variables, only the 71% increase in ES/BS in the particle treated group compared to the control group ($p = 0.004$) met the Bonferroni criteria for significance of $p < 0.0125$ (i.e., 0.05/4, since there were four variables of interest) (Table 1). There was a tendency to have lower BV/TV (39%) and QS/BS (4%), but these differences were not significant when adjusting for multiple comparisons. There was no difference in Ob.S/BS. TRAP positive cells were detected at the bone-implant interface in 5 of 10 particle-treated rats and 2 of 10 control rats ($p = 0.35$, Fig. 6). For rats with TRAP positive cells at the bone-implant interface, the number of such cells was higher for the particle-treated group than the control group, but the difference was not statistically significant: 21.2 (± 10.2) versus 3.0 (± 0.0) ($p = 0.051$).

Serum biomarkers

The serum level of CTX-I in the particle-treated group was 23 times higher than that in the control group (Table 1, p=0.004). The OC level for 5 rats was lower than the detection limit of 50 ng/ml and therefore the values were set at one-half the detection limit (25 ng/ml). The serum level of OC in the particle-treated group was 85% lower than that in the control group (Table 1, p=0.004). Both of these values met the criteria for significance after adjusting for multiple comparisons ($p < 0.025$, since there were two comparisons of interest).

Correlation between mechanical pull-out testing variables and other variables

A number of variables were correlated with the interface mechanics (Table 2). The strongest correlation for both strength and energy to yield was with serum OC (Fig. 7). Implant fixation strength was also positively correlated with BV/TV, Conn.D., and body weight gain, and was negatively correlated with serum CTX-I. Implant pull-out energy to yield was also positively correlated with body weight gain, and negatively correlated with the number of TRAP positive cells and ES/BS. Interface stiffness was positively correlated with body weight gain while energy to failure was not significantly correlated with any of the other variables.

DISCUSSION

The current study demonstrates for the first time that LPS-doped PE particles alter serum biomarkers of bone turnover and peri-implant static histomorphometric indices of bone remodeling in a model with demonstrated implant loosening. We also examined other variables, including planar radiographic and three-dimensional micro computed tomographic characterization of peri-implant bone volume and architecture, histology, and histochemistry to place the study in context. All the endpoints showed significant effects, consistent with induced bone loss at the bone-implant interface and within the surrounding trabecular bone bed and depressed implant fixation. We found no effect on trabecular bone volume at a site

remote from the location of the implant placement. In addition, we found that weight gain in the particle-treated animals was diminished beginning at 6 weeks.

Because adherent endotoxin increases the bioactivity of particles [6,32–34] and endotoxin is often present on implant materials [35], we used LPS-doped particles rather than untreated particles to induce implant loosening in our model. During preparation of the LPS-doped particles, we removed the unbound LPS by repeated washings to exclude the effect of free endotoxin in the model. The use of LPS-doped PE particles has been shown to lead to less bone-implant attachment than the use of non-doped particles in a rat model, although the "clean" particles also caused less attachment than the no particle controls [34]. Thus, it is likely that the use of LPS-doped particles represents an accelerated model of implant loosening.

Aseptic loosening implies lack of infection as judged by clinical or microbiological criteria [5]. Thus, one may question whether or not the use of LPS-doped particles constitutes a model of aseptic loosening since LPS is a bacterial cell wall molecule. It is known that LPS can be present in periprosthetic tissue of patients with loosened implants but in whom there is no clinical or microbiological evidence of infection [36]. Endotoxin contamination of orthopedic implants and wear debris is common and appears to be an important component of biological activity [37]. In our study, there was no bacteriological evidence of infection, suggesting that this can be considered a model of aseptic loosening.

A potential confounding factor in interpreting the biomarker data from the present study is that systemic distribution of LPS could affect bone metabolism and serum biomarkers of bone turnover. Chronic exposure to LPS (total dose of approximately 1.1×10^4 μg LPS/kg over a 12 week period, our calculation) via a slow release pellet in a rat model led to a 7% decrease in bone mineral content of the femur, no changes in serum osteocalcin and a doubling in serum tartrate resistant acid phosphatase [38]. Intraperitoneal injection of free LPS was associated with diminished BV/TV [39], in which the total exposure was approximately 10^4 μg LPS/kg over a 4 to 6 week period in a mouse model. Bone biomarker data are not available from that study, but presumably would have shown elevated resorption. In our study, the maximum possible exposure was ~1.71 μg LPS/kg since each rat received a total of 0.77 μg LPS over the 12 week course of the study and the rats were approximately 450 g. Thus, the likely systemic exposure in our study was at least three orders of magnitude lower than in the systemic administration models with skeletal effects. In addition, we did not find evidence of a difference in trabecular BV/TV at a remote site. Consistent with our observation, in the study of Xing et al [34] using a model similar to the one reported here, one of the groups received intraperitoneal administration of LPS (total dose of ~0.55 μg LPS/kg over a 6 week period, our calculation), and there also was no evidence of an effect on bone density at a remote site. Thus, our interpretation of the serum biomarker data is that the LPS-doped particles caused inflammation both within the knee joint and in the tissue adjacent to the implant, leading to elevated peri-implant bone resorption, decreased bone volume, deteriorated trabecular architecture and diminished implant fixation with corollary effects on serum biomarkers of bone formation and bone resorption.

It is also possible that the decreased weight gain in the rats injected with LPS-doped particles indirectly affected the bone biomarker data. In the study by Shen et al. described in the previous paragraph [38], the authors observed no effect of LPS administration on body weight gain during the 12 week course of their study. However, systemic administration of LPS via injection into the intraperitoneal cavity has been reported to have a transient effect on body weight [40]. Strassmann et al. reported that free LPS administered intraperitoneally in a single bolus in mice at a dose of approximately 1.5×10^4 μg LPS/kg (our calculation) induced a transient weight loss at 24 to 72 hours but the weight had normalized by 96

hours [40]. The total exposure in our model (~ 1.71 μg/kg over a 12 week period, see above) was at least 4 orders of magnitude less than in the study that observed only a brief transient effect of LPS on body weight. Thus, based on these two studies [38,40], it seems unlikely that the LPS administered in our study had an effect on body weight. Even if we accept that the relatively low level of exposure in our experiment caused the diminished weight gain, a recent study showed that differential weight gain on the order of magnitude observed in the present study had no effect on bone metabolism or structure [41]. Our interpretation of the data is that the diminished weight gain was most likely a secondary effect of the local LPS-doped particle induced inflammation of the joint and peri-implant region. To our knowledge, other groups have not reported on animal weight in models of particle-induced osteolysis. The relationship between body weight and particle-induced implant loosening may merit further attention.

In the clinic, particle-induced peri-prosthetic osteolysis is a long term net bone resorptive process which precedes loosening. The detection of early inflammatory reaction and osteolysis before the occurrence of observable loosening is a challenge. Biochemical markers of bone turnover in the serum or urine could be useful indicators to reflect changes of bone metabolism. In the current study, we found an increased level of CTX-I and a decreased level of OC in the sera of particle-treated rats. In addition, mechanical fixation was positively correlated with serum OC level, and negatively correlated with serum CTX-I level. Most clinical studies demonstrated that patients with implant loosening and peri-prosthetic osteolysis had elevated levels of biomarkers of bone resorption [18–23]. One study using a murine calvarial model of osteolysis demonstrated an increased level of TRAP-5b [37] in the serum of mice treated with particles. Thus, our finding of elevated CTX-I, a biomarker for bone resorption, is consistent with reports in the literature, and is the first such report in an animal model of implant fixation. The findings for biomarkers of bone formation in patients with aseptic loosening and peri-prosthetic osteolysis are inconsistent. One study demonstrated decreased carboxyterminal propeptide of type I procollagen (PICP) in the serum of patients with loosened implants [20], similar to our finding of decreased serum OC. However, other studies in patients with unstable implants showed elevated levels of serum OC [19,21] or unchanged serum OC [23] and PICP [19]. We are not aware of any previous study of bone formation markers in an animal model of implant fixation. Together with our data which showed significant correlations between the biomarkers and fixation mechanics, these studies indicate that serum biomarkers of bone turnover may be a good indicator of the fixation status of the implant.

We report here the first histomorphometric characterization of the peri-implant bone surfaces in an animal model of induced implant loosening. We found that the particles increased eroded surface, implying elevated bone resorption. In vitro studies have found that wear particles not only stimulate the production of bone resorptive cytokines [2], but also significantly suppress the expression of procollagen-α1 [42] and synthesis of type I collagen [43] from osteoblasts. In vivo studies using different animal models demonstrated that the presence of polyethylene particles increased osteoclast-like cells [14,44]. One animal study demonstrated that polyethylene particles not only enhanced bone resorption in vivo, but also inhibited the expression of collagen, glycosaminoglycan and transforming growth factor-β in vivo, which probably reflects depressed bioactivity of osteoblasts [45]. Therefore, the static histomorphometry findings of the present study are consistent with current knowledge of the effects of wear particles on the catabolic aspects of bone turnover. Although the non-significant trend of increased bone forming surface relative to total bone surface in the peri-implant region seems to contradict the decreased OC level found in the serum, it is likely that the absolute amount of bone forming surface in the particle-treated group was actually less because the total bone surface was decreased. Future studies, in which double fluorochrome labels are administered, are needed to determine if osteoblastic

activity differs between control and particle-treated animals. In addition, the lack of effect on remote site trabecular bone volume suggests that the LPS-doped particle effects on bone remodeling were only local and did not have a generalized effect on the skeleton.

In the current literature, the effect of particles on mechanical fixation of implants has only been reported in two studies using rat models [11,16]. In the present study, we demonstrated decreased implant fixation strength and decreased energy to failure of implants in the particle-treated group. Neither our study nor the previous studies included multiple time points, so the time course of the depressed fixation is not certain. Thus, we cannot rule out that the depressed fixation in our model or the previous reports may be due to failure to achieve initial fixation.

Additional histological findings in the particle-treated group of the present study include (1) the presence of a synovial-like membrane containing a large number of PE particles at the bone-implant interface, (2) more samples with TRAP positive cells at the bone-implant interface, and (3) the presence of a synovial-like tissue on the surface of the distal femoral articular cartilage. The synovial-like membrane at the interface was initially described in patients with loose hip replacements and was found to include many macrophages and giant cells [12], suggesting its key role in bone resorption. A similar histological structure was also detected at the bone-cement or bone-implant interface in several rat models with the presence of wear particles [8,13,14]. Osteoclast-like cells adjacent to resorbed bone were confirmed by TRAP staining in one study using an osteolysis model in the rat [14]. The synovial-like tissue on the surface of the articular cartilage, which has not been described in other models of particle-induced implant loosening, is very similar to pannus tissue in rheumatoid arthritis [46], which is believed to be derived from the synovial membrane of the knee joint capsule. This similarity suggests that the synovial membrane of the joint capsule may play a role in mediating the effects of particulate debris.

μCT evaluation, including bone volume and bone density, has been widely used to evaluate the effects of particles in models of osteolysis or aseptic loosening [10,11,34,37,47,48], but these studies have not reported on alterations in trabecular architecture. In our study, we assessed the region between the endocortical surface and implant surface and found a significant decrease in trabecular bone volume and connectivity density in the particle-treated group adjacent to the distal 3 mm of the implant. In the murine calvarium model of osteolysis, particles usually lead to higher μCT bone resorption volume [37,47,48], i.e., volumes of interest largely devoid of bone. In the studies using animal models of intramedullary implantation, μCT evaluation demonstrated decreased peri-prosthetic bone volume [11] and inferred bone-implant contact [10,34] after the administration of particles. Our findings are consistent with these previous reports and provide new data on tissue-level mechanisms explaining the depressed implant fixation (decreased connectivity density, implying loss of trabeculae and trabecular connections). In addition, the current study also showed that μCT trabecular bone volume and connectivity density were positively correlated with implant fixation strength. This finding confirms that endocortical implant anchorage is critically dependent on μCT peri-implant bone architecture [49].

CONCLUSION

In this study, we demonstrated that LPS-doped PE particles induced differences in serum biomarkers and peri-implant histomorphometric findings consistent with increased bone resorption and depressed bone formation in a rat model of depressed implant fixation.

Acknowledgments

Lou Fogg, PhD provided statistical advice. Nadim Hallab, PhD provided access to the mechanical testing machine. Josh Jacobs, MD provided useful comments. Technical help was provided by Dana Glock, Arihiko Kanaji, MD and David Karwo. Support was also provided through the Rush microCT/Histology Core Facility. Funding was provided by the Grainger Foundation and NIH Grant R21AR054171.

Reference List

1. Kurtz S, Ong K, Lau E, Mowat F, Halpern M. Projections of primary and revision hip and knee arthroplasty in the United States from 2005 to 2030. J Bone Joint Surg Am. 2007; 89:780–785. [PubMed: 17403800]
2. Glant TT, Jacobs JJ, Molnar G, Shanbhag AS, Valyon M, Galante JO. Bone resorption activity of particulate-stimulated macrophages. J Bone Miner Res. 1993; 8:1071–1079. [PubMed: 8237476]
3. Jacobs, JJ.; Goodman, SB.; Sumner, DR.; Hallab, NJ. Biological response to orthopaedic implants. In: Buckwalter, JA.; Einhorn, TA.; Simon, SR., editors. Orthopaedic Basic Science. Rosemont, Illinois: American Academy of Orthopaedic Surgeons; 2000. p. 401-426.
4. Willert HG, Bertram H, Buchhorn GH. Osteolysis in alloarthroplasty of the hip. The role of ultra-high molecular weight polyethylene wear particles. Clin Orthop. 1990; 258:95–107. [PubMed: 2203577]
5. Tatro JM, Taki N, Islam AS, Goldberg VM, Rimnac CM, Doerschuk CM, Stewart MC, Greenfield EM. The balance between endotoxin accumulation and clearance during particle-induced osteolysis in murine calvaria. J Orthop Res. 2007; 25:361–369. [PubMed: 17106883]
6. Skoglund B, Larsson L, Aspenberg PA. Bone-resorptive effects of endotoxin-contaminated high-density polyethylene particles spontaneously eliminated in vivo. J Bone Joint Surg Br. 2002; 84:767–773. [PubMed: 12188502]
7. Gruen TA, McNeice GM, Amstutz HC. Modes of failure of cemented stem-type femoral components: a radiographic analysis of loosening. Clin Orthop. 1979; 141:17–27. [PubMed: 477100]
8. Howie DW, Vernon-Roberts B, Oakeshott R, Manthey B. A rat model of resorption of bone at the cement-bone interface in the presence of polyethylene wear particles. J Bone Joint Surg Am. 1988; 70:257–263. [PubMed: 3257760]
9. Venesmaa PK, Kroger HP, Miettinen HJ, Jurvelin JS, Suomalainen OT, Alhav EM. Alendronate reduces periprosthetic bone loss after uncemented primary total hip arthroplasty: a prospective randomized study. J Bone Miner Res. 2001; 16:2126–2131. [PubMed: 11697810]
10. Xing Z, Hasty KA, Smith RA. Administration of pamidronate alters bone-titanium attachment in the presence of endotoxin-coated polyethylene particles. J Biomed Mater Res B Appl Biomater. 2006; 83:354–358. [PubMed: 17385218]
11. Suratwala SJ, Cho SK, Van Raalte JJ, Park SH, Seo SW, Chang SS, Gardner TR, Lee FY. Enhancement of periprosthetic bone quality with topical hydroxyapatite-bisphosphonate composite. J Bone Joint Surg Am. 2008; 90:2189–2196. [PubMed: 18829917]
12. Goldring SR, Schiller AL, Roelke M, Rourke CM, O'Neill DA, Harris WH. The synovial-like membrane at the bone-cement interface in loose total hip replacements and it proposed role in bone lysis. J Bone Joint Surg. 1983; 65-A:575–584. [PubMed: 6304106]
13. Allen M, Brett F, Millett P, Rushton N. The effects of particulate polyethylene at a weight-bearing bone-implant interface. A study in rats. J Bone Joint Surg Br. 1996; 78:32–37. [PubMed: 8898123]
14. Kim KJ, Kobayashi Y, Itoh T. Osteolysis model with continuous infusion of polyethylene particles. Clin Orthop Relat Res. 1998; 352:46–52. [PubMed: 9678032]
15. Ryd L, Albrektsson BEJ, Carlsson L, Dansgard F, Herberts P, Lindstraand A, Regner L, Toksvig-Larsen S. Roentgen stereophotogrammetric analysis as a predictor of mechanical loosening knee prostheses. J Bone Joint Surg. 1995; 77:377–383.
16. Smith RA, Maghsoodpoour A, Hallab NJ. In vivo response to cross-linked polyethylene and polycarbonate-urethane particles. J Biomed Mater Res A. 2010; 93:227–234. [PubMed: 19557792]

17. Yang SY, Yu H, Gong W, Wu B, Mayton L, Costello R, Wooley PH. Murine model of prosthesis failure for the long-term study of aseptic loosening. J Orthop Res. 2007; 25:603–611. [PubMed: 17278141]
18. Antoniou J, Huk O, Zukor D, Eyre D, Alini M. Collagen crosslinked N-telopeptides as markers for evaluating particulate osteolysis: a preliminary study. J Orthop Res. 2000; 18:64–67. [PubMed: 10716280]
19. Li MG, Thorsen K, Nilsson KG. Increased bone turnover as reflected by biochemical markers in patients with potentially unstable fixation of the tibial component. Arch Orthop Trauma Surg. 2004; 124:404–409. [PubMed: 15156331]
20. Savarino L, Granchi D, Cenni E, Baldini N, Greco M, Giunti A. Systemic cross-linked N-terminal telopeptide and procollagen I C-terminal extension peptide as markers of bone turnover after total hip arthroplasty. J Bone Joint Surg Br. 2005; 87:571–576. [PubMed: 15795214]
21. Schneider U, Breusch SJ, Termath S, Thomsen M, Brocai DRC, Niethard F-U, Kasperk C. Increased urinary crosslink levels in aseptic loosening of total hip arthroplasty. J Arthrop. 1998; 13:687–692.
22. von Schewelov T, Carlsson A, Dahlberg L. Cross-linked N-telopeptide of type I collagen (NTx) in urine as a predictor of periprosthetic osteolysis. J Orthop Res. 2006; 24:1342–1348. [PubMed: 16718682]
23. Wilkinson JM, Hamer AJ, Rogers A, Stockley I, Eastell R. Bone mineral density and biochemical markers of bone turnover in aseptic loosening after total hip arthroplasty. J Orthop Res. 2003; 21:691–696. [PubMed: 12798070]
24. Barber TA, Golledge SL, Castner DG, Healy KE. Peptide-modified p(AAm-co-EG/AAc) IPNs grafted to bulk titanium modulate osteoblast behavior in vitro. J Biomed Mater Res. 2003; 64:38–47.
25. Taki N, Tatro JM, Nalepka JL, Togawa D, Goldberg VM, Rimnac CM, Greenfield EM. Polyethylene and titanium particles induce osteolysis by similar, lymphocyte-independent, mechanisms. J Orthop Res. 2005; 23:376–383. [PubMed: 15734251]
26. Petsch D, Anspach FB. Endotoxin removal from protein solutions. J Biotechnol. 2000; 76:97–119. [PubMed: 10656326]
27. Liu S, Broucek J, Virdi AS, Sumner DR. Limitations of using micro-computed tomography to predict bone-implant contact and mechanical fixation. Journal of Microscopy. 2011 (in press).
28. Bouxsein ML, Boyd SK, Christiansen BA, Guldberg RE, Jepsen KJ, Muller R. Guidelines for assessment of bone microstructure in rodents using micro-computed tomography. J Bone Miner Res. 2010; 25:1468–1486. [PubMed: 20533309]
29. Parfitt AM, Drezner MK, Glorieux FH, Kanis JA, Malluche H, Meunier PJ, Ott SM, Recker RR. Bone histomorphometry: standardization of nomenclature, symbols, and units. J Bone Miner Res. 1987; 2:595–610. [PubMed: 3455637]
30. Kuroda S, Virdi AS, Li P, Healy KE, Sumner DR. A low temperature biomimetic calcium phosphate surface enhances early implant fixation in a rat model. J Biomed Mater Res. 2004; 70A: 66–73.
31. Berzins, A.; Sumner, DR. Implant pushout and pullout tests. In: An, YH.; Draughn, RA., editors. Mechanical testing of bone and the bone-implant interface. Boca Raton: CRC Press; 2000. p. 463-476.
32. Bi Y, Seabold JM, Kaar SG, Ragab AA, Goldberg VM, Anderson JM, Greenfield EM. Adherent endotoxin on orthopedic wear particles stimulates cytokine production and osteoclast differentiation. J Bone Miner Res. 2001; 16:2082–2091. [PubMed: 11697805]
33. Ragab AA, Van De Motter RR, Lavish SA, Goldberg VM, Ninomiya T, Carlin CR, Greenfield EM. Measurement and removal of adherent endotoxin from titanium particles and implant surfaces. J Orthop Res. 1999; 17:803–809. [PubMed: 10632445]
34. Xing Z, Pabst MJ, Hasty KA, Smith RA. Accumulation of LPS by polyethylene particles decreases bone attachment to implants. J Orthop Res. 2006; 24:959–966. [PubMed: 16609962]
35. Greenfield EM, Bi Y, Ragab AA, Goldberg VM, Nalepka JL, Seabold JM. Does endotoxin contribute to aseptic loosening of orthopedic implants? J Biomed Mater Res B Appl Biomater. 2005; 72:179–185. [PubMed: 15449253]

36. Nalepka JL, Lee MJ, Kraay MJ, Marcus RE, Goldberg VM, Chen X, Greenfield EM. Lipopolysaccharide found in aseptic loosening of patients with inflammatory arthritis. Clin Orthop Relat Res. 2006; 451:229–235. [PubMed: 16735873]
37. Landgraeber S, Jaeckel S, Loer F, Wedemeyer C, Hilken G, Canbay A, Totsch M, von Knoch M. Pan-caspase inhibition suppresses polyethylene particle-induced osteolysis. Apoptosis. 2009; 14:173–81. [PubMed: 19130234]
38. Shen C-L, Yeh JK, Cao JJ, Tatum OL, Dagda RY, Wang J-S. Synergistic effects of green tea polyphenols and alphacalcidol on chronic inflammation-induced bone loss in female rats. Osteoporos Int. 2010; 21:1841–1852. [PubMed: 20069278]
39. Esplin BL, Shimazu T, Welner RS, Garrett KP, Nie L, Zhang Q, Humphrey MB, Yang Q, Borghesi LA, Kincade PW. Chronic exposure to a TLR ligand injures hematopoietic stem cells. J Immunol. 2011; 186:5367–5375. [PubMed: 21441445]
40. Strassmann G, Fong M, Windsor S, Neta R. The role of interleukin-6 in lipopolysaccharide-induced weight loss, hypoglycemia and fibrinogen production, in vivo. Cytokine. 1993; 5:285–290. [PubMed: 8260592]
41. Turner RT, Iwaniec UT. Moderate weight gain does not influence bone metabolism in skeletally mature female rats. Bone. 2010; 47:631–635. [PubMed: 20601291]
42. Yao J, Glant TT, Lark MW, Mikecz K, Jacobs JJ, Hutchinson NI, Hoerrner LA, Kuetner KE, Galante JO. The potential role of fibroblasts in periprosthetic osteolysis: fibroblast response to titanium particles. J Bone Miner Res. 1995; 10:1417–1427. [PubMed: 7502715]
43. Vermes C, Roebuck KA, Chandrasekaran R, Dobai JG, Jacobs JJ, Glant TT. Particulate wear debris activates protein tyrosine kinases and nuclear factor kappaB, which down-regulates type I collagen synthesis in human osteoblasts. J Bone Miner Res. 2000; 15:1756–1765. [PubMed: 10976995]
44. Goodman SB, Song Y, Chun L, Regula D, Aspenberg P. Effects of TGFbeta on bone ingrowth in the presence of polyethylene particles. J Bone Joint Surg. 1999; 81:1069–1075.
45. Sacomen D, Smith RL, Song Y, Fornasier V, Goodman SB. Effects of polyethylene particles on tissue surrounding knee arthroplasties in rabbits. J Biomed Mater Res. 1998; 43:123–130. [PubMed: 9619430]
46. Allard SA, Muirden KD, Maini RN. Correlation of histopathological features of pannus with patterns of damage in different joints in rheumatoid arthritis. Ann Rheum Dis. 1991; 50:278–283. [PubMed: 2042980]
47. Markel DC, Zhang R, Shi T, Hawkins M, Ren W. Inhibitory effects of erythromycin on wear debris-induced VEGF/Flt-1 gene production and osteolysis. Inflamm Res. 2009; 58:413–421. [PubMed: 19262986]
48. Tsutsumi R, Hock C, Bechtold CD, Proulx ST, Bukata SV, Ito H, Awad A, Nakamura T, O'Keefe RJ, Schwarz EM. Differential effects of biologic versus bisphosphonate inhibition of wear debris-induced osteolysis assessed by longitudinal micro-CT. J Orthop Res. 2008; 26:1340–1346. [PubMed: 18404739]
49. Gabet Y, Kohavi D, Voide R, Mueller TL, Muller R, Bab I. Endosseous implant anchorage is critically dependent on mechanostructural determinants of peri-implant bone trabeculae. J Bone Miner Res. 2010; 25:575–583. [PubMed: 19653813]

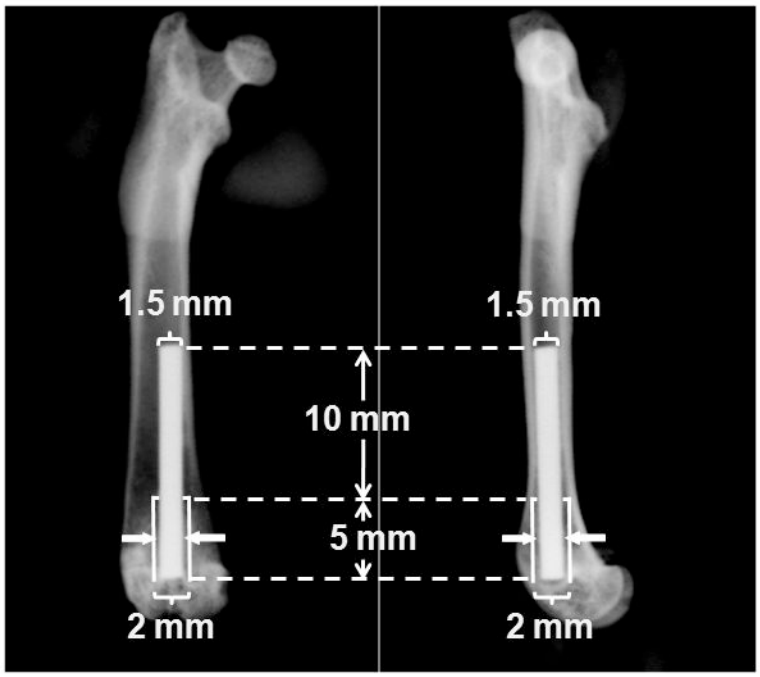

Figure 1.
Illustration of implant placement in the model. A 15 mm long by 1.5 mm diameter titanium implant was press fit in the distal end of the femur through the knee joint. A 0.25 mm wide gap (solid arrows) was created around the distal 5 mm of the implant, leaving good initial fixation at the proximal 10 mm of the implant.

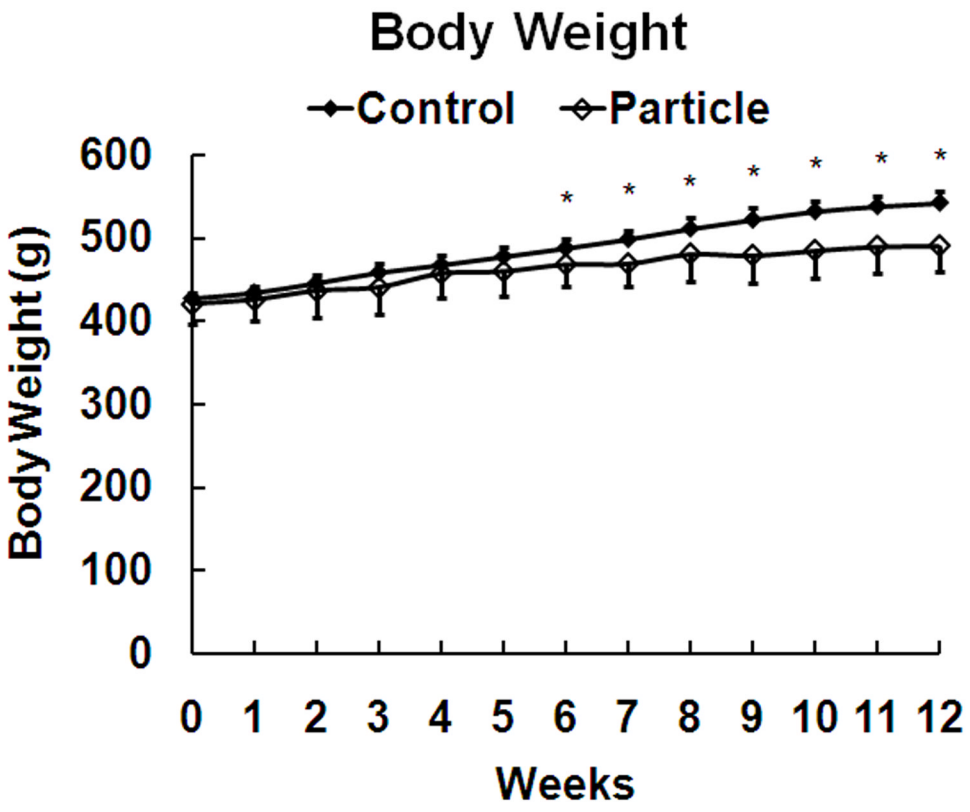

Figure 2.
Body weight at weekly intervals (means and standard deviations), * $p < 0.05$ compared to control.

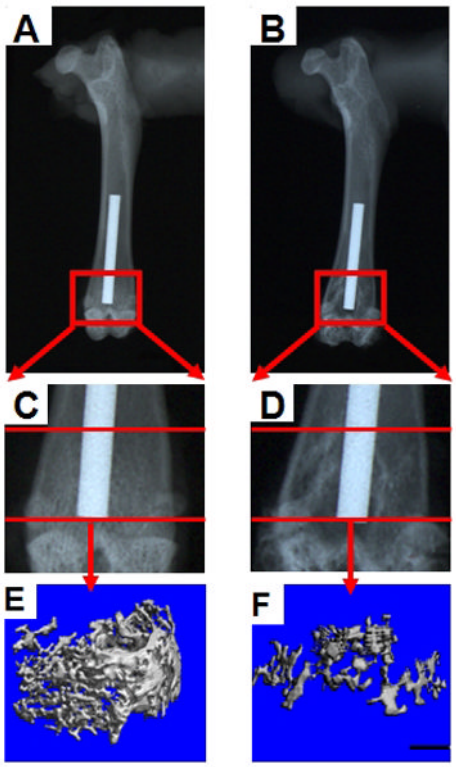

Figure 3.
X-ray images of a control sample (A, C, and E) and a particle-treated sample (B, D, and F). Peri-implant radiolucent areas were present more often at the distal end of implant in the particle-treated group than in the control group. The three-dimensional trabecular bone renderings from μCT of the entire region between the endocortical surface and the implant show less bone adjacent to the distal one-third of the implant in a rat treated with particles (F) than in the control rat (E). Note that the implant is not shown in these three-dimensional reconstructions. Scale bar is 1mm (panels E and F).

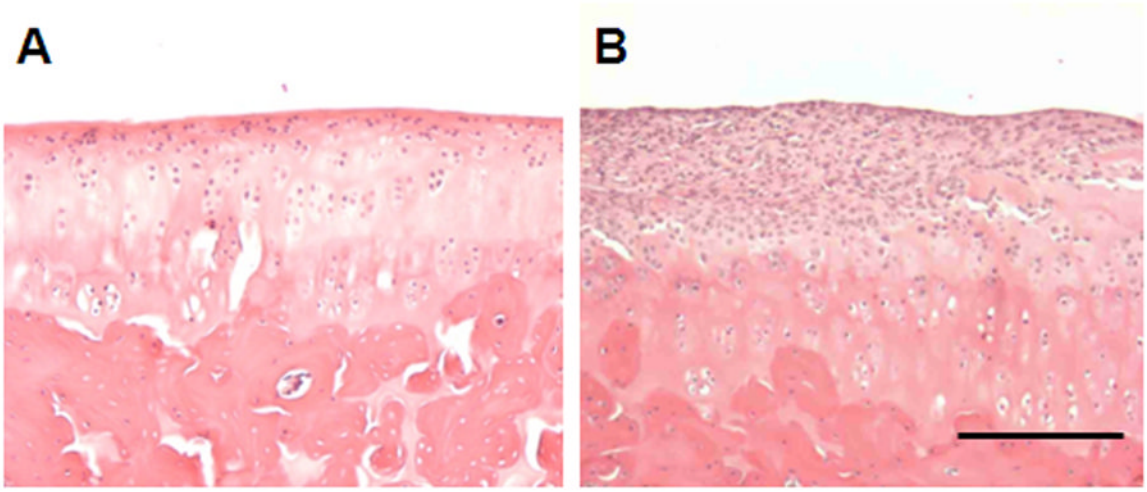

Figure 4.
Images show the articular cartilage of the distal femur from animals in the control group (A) and the particle-treated group (B). Synovial-like tissue always covered a portion of the surface of the articular cartilage in the particle-treated group. H&E staining. Scale bar is 100 μm.

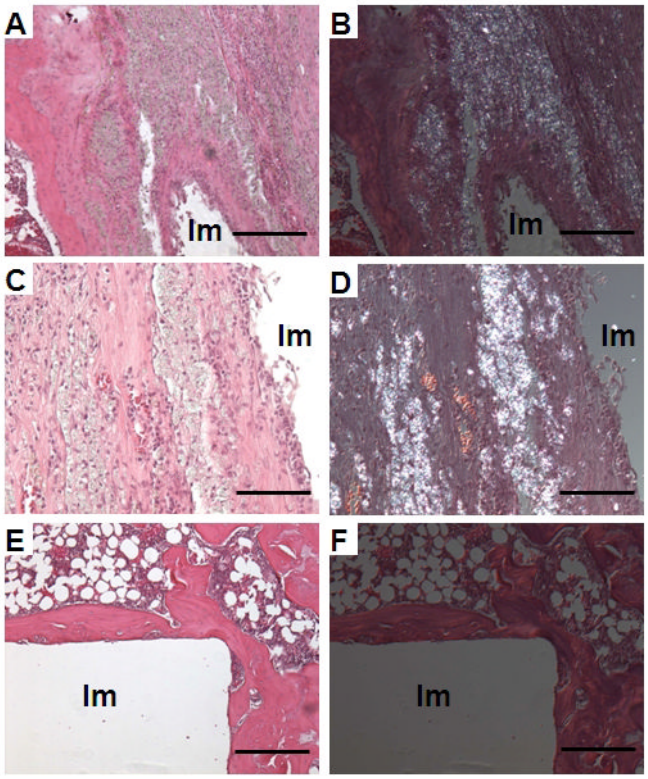

Figure 5.
Images show H&E staining under normal light (A, C, E) and under polarized light (B, D, F). Note the presence of a thick synovial-like membrane at the implant interface (A, C), associated with birefringent particles (B, D) in the particle-treated group. Samples in the control group showed a thick and even layer of peri-implant bone without a membrane at the bone-implant interface and a lack of birefringent particles (E, F). Scale bars in image A, B, E and F are 250 μm. Scale bars in image C and D are 50 μm. Im: Empty space after removing the implant.

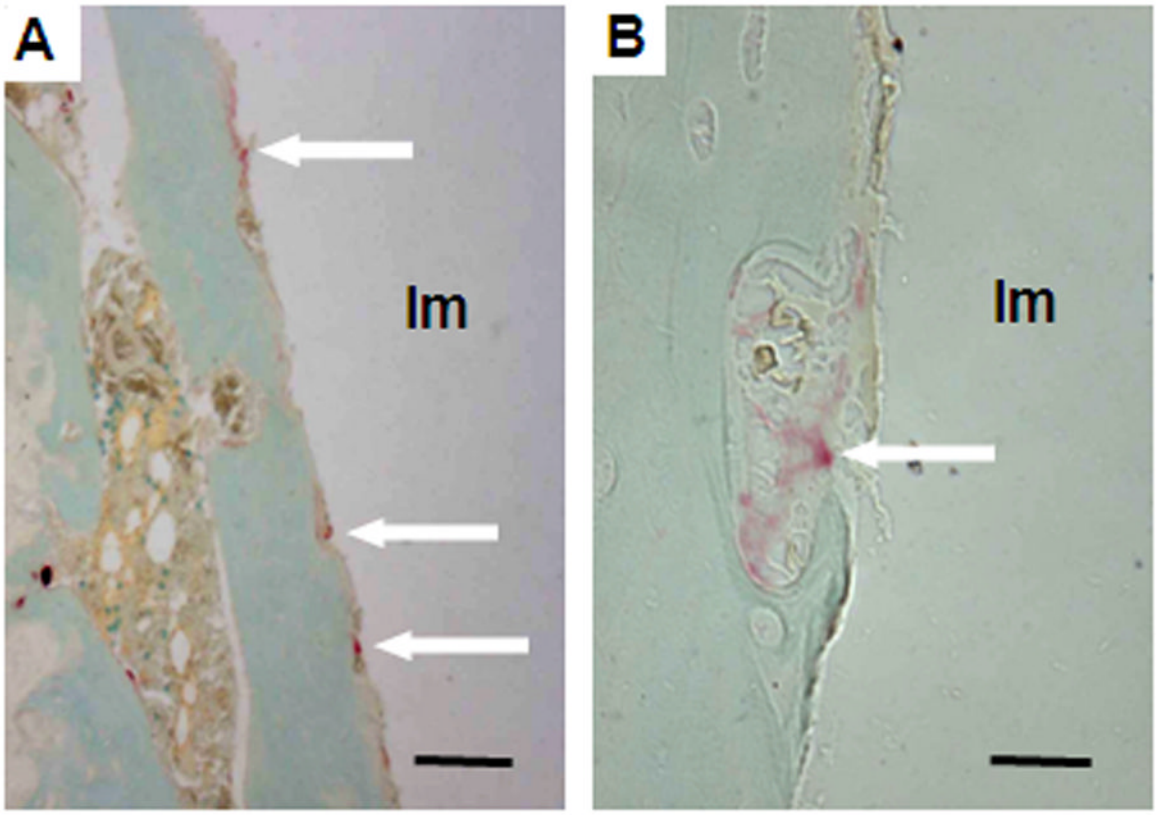

Figure 6.
Images show TRAP positive stained cells (arrows) at the bone-implant interface of a sample in the particle-treated group. A: Scale bar is 100 μm. B: Scale bar is 10μm. Im: Implant space.

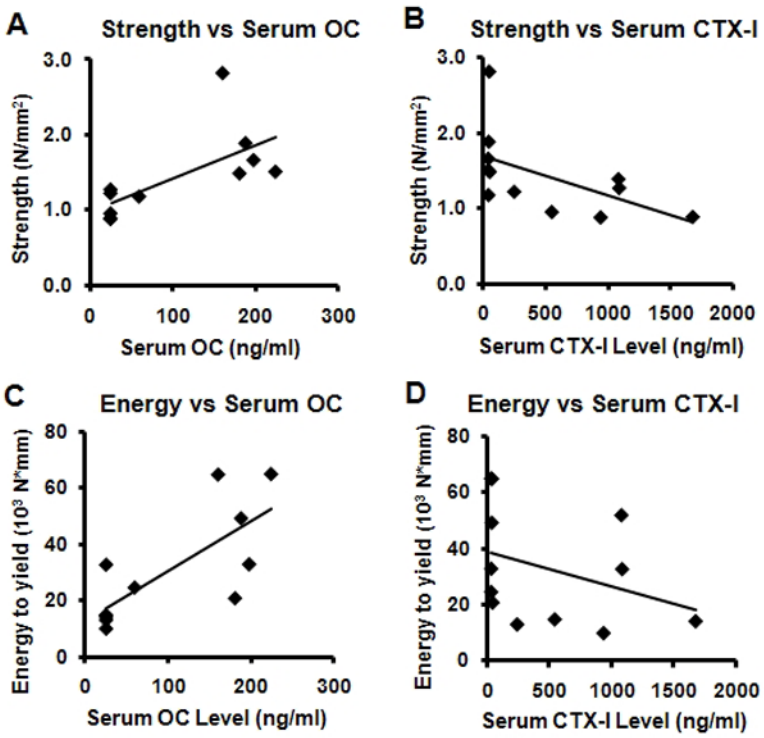

Figure 7.

Scatter plots with linear regression lines. A: strength v. OC Level, B: strength v. CTX-I Level, C: energy to yield v. OC Level, and D: energy to yield v. CTX-I Level.

Table 1

Animal body weight, bone architecture data from μCT in ROI III, static bone histomorphometry in the endocortical area, mechanical pull-out testing measurements and serum bone turnover biomarkers for particle and control groups, mean (standard deviation).

Variable	Particle-Treated	Control	P-Value
Weight	(n = 12)	(n = 12)	
Weight at start of study	420.8 (23.9)	427.5 (6.2)	0.47
Weight at end of study	490.4 (31.9)	541.8 (14.4)	< 0.001*
Weight gain from start to end of study	69.6 (25.5)	114.3 (13.8)	< 0.001*
μCT (ROI III)	(n = 12)	(n = 12)	
BV/TV (%)	7.6 (2.7)	13.8 (3.6)	0.001*
Conn. D. (1/mm^3)	2.6 (1.6)	7.0 (3.0)	0.001*
Tb.N (1/mm)	1.0 (0.2)	1.2 (0.2)	0.043
Tb.Th (mm)	0.15 (0.02)	0.15 (0.01)	0.91
Tb.Sp (mm)	1.1 (0.2)	0.9 (0.2)	0.018
Static Histomorphometry	(n = 9)	(n = 9)	
Ob.S/BS (%)	7.2 (2.3)	5.8 (1.7)	0.23
ES/BS (%)	5.8 (1.4)	3.4 (0.8)	0.004*
QS/BS (%)	87.0 (3.6)	90.8 (2.3)	0.047
BV/TV (%)	7.5 (3.4)	12.2 (4.7)	0.017
Mechanical Pull-Out Testing	(n = 11)	(n = 11)	
Strength (N/mm^2)	1.0 (0.3)	1.7 (0.5)	< 0.001*
Energy to yield (N-mm)	83.4 (60.3)	168.6 (70.3)	0.004*
Stiffness (N/mm)	125.1 (53.5)	235.2 (144.0)	0.028
Energy to failure (N-mm)	120.4 (90.8)	211.2 (116.9)	0.053
Serum biomarkers			
CTX-I (ng/ml)	(n = 6) 928.5 (494.2)	(n = 6) 39.9 (4.7)	0.004*
Osteocalcin (ng/ml)	(n = 5) 25.0 (0.0)	(n = 6) 168.4 (57.3)	0.004*

*significant p value after Bonferroni correction for multiple tests

Table 2

Spearman correlations between mechanical testing variables and other variables: rho values and p values in parentheses are listed for each pair of compared variables * p<0.05, ** p<0.01).

	μCT BV/TV (n=22)	μCT Conn.D. (n=22)	OC Level (n=11)	CTX-I level (n=12)	TRAP(+)Number (n=18)	Ob.S/BS (n=16)	ES/BS (n=16)	Weight Gain (n=22)
Strength	0.440*	0.448*	0.763**	−0.601*	−0.397	−0.050	−0.488	0.638**
	(0.041)	(0.037)	(0.006)	(0.039)	(0.103)	(0.854)	(0.055)	(0.001)
Energy to yield	0.390	0.379	0.791**	−0.503	−0.498*	−0.221	−0.579*	0.563**
	(0.073)	(0.082)	(0.004)	(0.095)	(0.035)	(0.412)	(0.019)	(0.006)
Energy to failure	0.303	0.281	0.553	−0.503	−0.230	−0.006	−0.365	0.297
	(0.170)	(0.206)	(0.078)	(0.095)	(0.358)	(0.983)	(0.165)	(0.179)
Stiffness	0.194	0.208	0.267	−0.084	−0.059	0.091	−0.050	0.441*
	(0.388)	(0.352)	(0.427)	(0.795)	(0.817)	(0.737)	(0.854)	(0.040)